Interaction of HCl with Ice: Investigation of the Predicted Trihydrate, Hexahydrate, and Monolayer Regimes

Krishna L. Foster,[†,‡] M. A. Tolbert,[†,‡] and S. M. George*[,†]

Department of Chemistry and Biochemistry and CIRES, University of Colorado, Boulder, Colorado 80309

Received: March 3, 1997; In Final Form: May 8, 1997[⊗]

Knowledge of the interaction of hydrogen chloride (HCl) with ice is important for an understanding of heterogeneous reactions on polar stratospheric clouds. The interaction of HCl with ice as a function of ice temperature, HCl partial pressure, and ice film thickness was studied using laser-induced thermal desorption (LITD) techniques. Ice films were prepared by depositing H_2O vapor onto a cooled Al_2O_3 substrate. The ice was then exposed to HCl partial pressures ranging from 1×10^{-9} to 1×10^{-6} Torr at ice temperatures from 140 to 186 K. HCl uptake by ice was monitored as a function of time using the HCl LITD signals. A doubly differentially pumped mass spectrometer allowed the LITD studies to be conducted at H_2O partial pressures up to 1×10^{-4} Torr. These high H_2O partial pressures are required to maintain stable ice films at the higher ice temperatures. At temperatures below 148 K, the HCl and H_2O LITD signals indicated that the ice films rapidly formed an $HCl{\cdot}3H_2O$ trihydrate film. Between 148 and 175 K, the HCl:H_2O ratio changed continuously with no observed stable $HCl{\cdot}6H_2O$ hexahydrate. At stratospheric temperatures between 180 and 186 K, HCl uptake on ice varied from 4×10^{14} to 2×10^{16} molecules/cm^2. This variation was attributed to varying ice surface roughness with the roughest ice films displaying the highest HCl uptake. HCl uptake was limited to ~1 ML (1 ML = 1.15×10^{15} molecules/cm^2) on the smoothest ice films, in agreement with previous estimates of monolayer HCl uptake by stratospheric ice.

1. Introduction

Chlorine activation by heterogeneous reactions on polar stratospheric clouds (PSCs) plays a critical role in polar ozone depletion.[1,2] PSCs are thought to be composed of nitric acid/ice mixtures (type I) or pure ice (type II). The present study focuses on type II PSCs that form at approximately 187 K in the polar stratosphere.[3] A strong correlation between midwinter ozone depletion and dehydration[4] suggests an important role for type II PSCs in polar ozone depletion.

An important mechanism for chlorine activation in the polar stratosphere is the heterogeneous reaction[5]

$$ClONO_2 + HCl \xrightarrow{PSC} Cl_2 + HNO_3 \qquad (1)$$

This reaction is efficient on water ice and HNO_3/ice surfaces and is very slow in the gas phase.[6−10] Although the reaction is known to be important, a detailed understanding of the heterogeneous reaction mechanism on PSCs is still lacking. A first step in unraveling the reaction mechanism is to probe the interaction of HCl with ice.

Several previous thermodynamic and kinetic studies have explored the interaction of HCl with ice. The HCl/H_2O phase diagram has been generated from experimental data and thermodynamic calculations. Figure 1 shows the phase diagram for HCl and ice as a function of HCl vapor pressure and temperature.[11] Depending on the conditions, HCl and H_2O are predicted to form HCl trihydrate ($HCl{\cdot}3H_2O$), HCl hexahydrate ($HCl{\cdot}6H_2O$), or supercooled liquid solutions.

The dotted region in Figure 1 highlights the range of HCl partial pressures and temperatures observed in the polar stratosphere. Stratospheric conditions are within the "ice" region

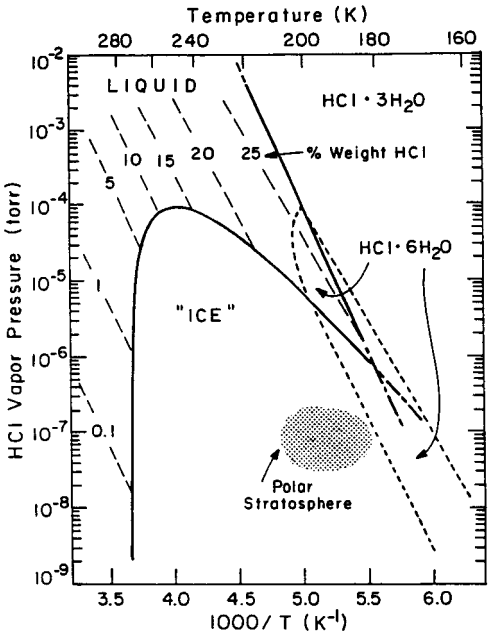

Figure 1. Phase diagram for HCl and ice as a function of HCl pressure and temperature. Reprinted with permission from ref 11. Copyright 1994 Blackwell Scientific.

of the phase diagram where the interaction of HCl with ice is expected to be limited to the ice surface.[11] However, polar stratospheric conditions occur close to several stable phases on the phase diagram. Because metastable phases can exist outside of phase boundaries, this study will focus on the behavior of HCl interacting with ice over a range of temperatures and pressures that includes the stratospheric environment.

Several theoretical studies have investigated the interaction of HCl with ice. Under the assumption that the HCl molecules do not dissociate on the ice surface, a maximum HCl surface coverage on ice was determined to be 10^{-7} monolayer (ML)

* To whom correspondence should be addressed.
† Department of Chemistry and Biochemistry.
‡ CIRES.
⊗ Abstract published in *Advance ACS Abstracts,* June 15, 1997.

S1089-5639(97)00772-X CCC: $14.00

under stratospheric conditions.[12] These calculations were extended to include HCl dissociation, and stable ions were formed on the ice surface.[13] Molecular dynamics simulations have also shown that HCl can ionize when a second bilayer of ice grows on top of the hydrogen-bonded HCl molecules as a result of the dynamic ice surface.[14,15] The ionized pair (H_3O^+ and Cl^-) is then incorporated into the ice surface.

Previous laboratory studies have also investigated the HCl coverage on ice under various conditions.[9,10,16−22] Ice films have been deposited on the walls of flow tubes and exposed to HCl gas.[9,10,18] The HCl surface coverage was inferred from the loss of gas phase HCl. These studies indicated that the HCl surface coverage is approximately one monolayer under stratospheric conditions.[9,10,18] The interaction of HCl with ice films has also been studied using other methods. Ice films exposed to HCl pressures of $10^{-7}-10^{-5}$ Torr at 155 K formed a thin layer on top of the ice film that was assigned as $HCl{\cdot}6H_2O$ by Fourier transform infrared (FTIR) spectroscopy.[17] Unfortunately, the amount of HCl in the ice film at 185 K was below the detection limit of transmission FTIR spectroscopy. Thin ice films were also exposed to HCl vapor at 120 K and investigated using temperature-programmed desorption (TPD) studies.[20] The formation of an $HCl{\cdot}6H_2O$ film was reported, and a monolayer of HCl was speculated to be present at the surface.

In the present study, the interaction of HCl with ice was studied at temperatures from 140 to 186 K and HCl partial pressures between 1×10^{-9} and 3×10^{-6} Torr. A doubly differentially pumped mass spectrometer allowed for H_2O partial pressures up to 1×10^{-4} Torr that are required to maintain stable ice films at the higher temperatures. According to the HCl and H_2O phase diagram, this range of temperatures and pressures includes the stability regions for HCl trihydrate ($HCl{\cdot}3H_2O$), HCl hexahydrate ($HCl{\cdot}6H_2O$), and ice. HCl was measured directly on the ice surface or in the ice films using laser-induced thermal desorption (LITD) techniques. Unlike the previous experimental studies, these LITD investigations could be performed at stratospheric conditions with submonolayer sensitivity. The LITD measurements explored the expected HCl trihydrate region, the predicted HCl hexahydrate region, and the HCl monolayer regime anticipated under stratospheric conditions.

2. Experimental Section

A. Vacuum Chamber and Double Differential Pumping. The experimental apparatus used to measure the interaction of HCl with ice is shown in Figure 2. An $Al_2O_3(0001)$ substrate was attached to a sample holder at the bottom of a cryostat and positioned in the center of an ultrahigh-vacuum chamber.[23,24] The Al_2O_3 substrate was a 0.5 mm thick single crystal with dimensions of 12×20 mm and a 5° wedge between the front and the back faces. The Al_2O_3 surface was cleaned using an O_2 plasma as described in previous work.[23] The chamber was pumped by a 190 L/s turbomolecular pump that produced a base pressure of 5×10^{-9} Torr. The chamber was equipped with a doubly differentially pumped mass spectrometer (UTI 100C), an ionization gauge, and an absolute capacitance manometer (MKS Baratron Type 690A.1 TRB) that can accurately measure pressures from 1×10^{-6} to 0.1 Torr.

The doubly differentially pumped region of the chamber containing the mass spectrometer is displayed in Figure 3. The mass spectrometer was separated from the main chamber by a glass shroud with an 8 mm diameter circular opening connecting the two regions. A copper cryopanel with a 25 mm circular opening was placed between the glass shroud and the mass spectrometer ionizer. The perimeter of the ionizer region of the mass spectrometer was covered with stainless steel foil to prevent electron currents between the ionizer and the nearby copper cryopanel.

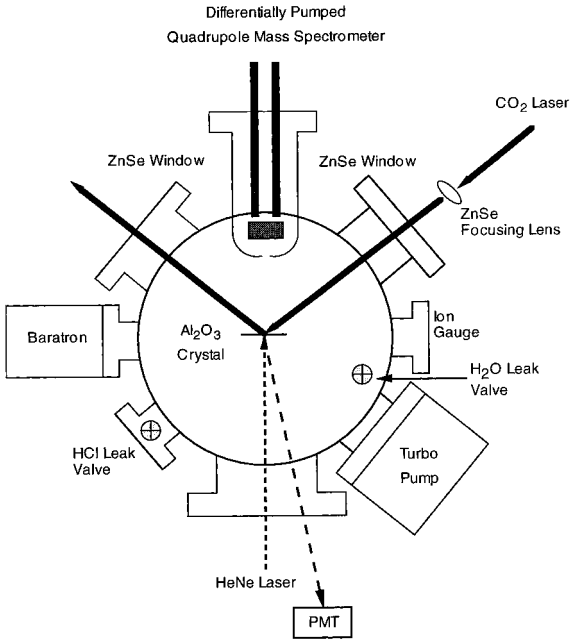

Figure 2. Schematic representation of the experimental apparatus.

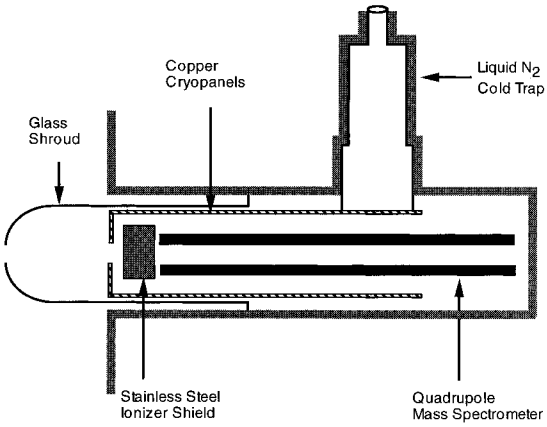

Figure 3. Schematic representation of the doubly differentially pumped mass spectrometer.

The copper cryopanel was in thermal contact with a liquid nitrogen-cooled trap as shown in Figure 3. The front face of the cryopanel was below 130 K during operation. This temperature is below the temperature of ≈160 K required for H_2O multilayer desorption into vacuum.[15] The sticking coefficient and condensation coefficient of H_2O on ice are both unity at $T < 140$ K.[25] Consequently, background H_2O molecules are cryogenically pumped by the cryopanel before they reach the ionizer of the mass spectrometer. The doubly differential pumping provided by the glass shroud and the cryopanel could sustain an H_2O pressure gradient of $\gtrsim 100$. This pressure differential allowed the ice film on the Al_2O_3 substrate to be exposed to stratospheric H_2O pressures of $\sim 10^{-4}$ Torr while maintaining H_2O pressures in the ionization region of $\lesssim 10^{-6}$ Torr.

B. Ice Film Preparation. For the experiments at the lower ice film temperatures between 140 and 175 K, the films were prepared by backfilling H_2O vapor into the chamber and onto the cooled Al_2O_3 substrate. For experiments at higher ice film temperatures where the H_2O multilayer desorption rate is substantial, some of the ice films were initially deposited at

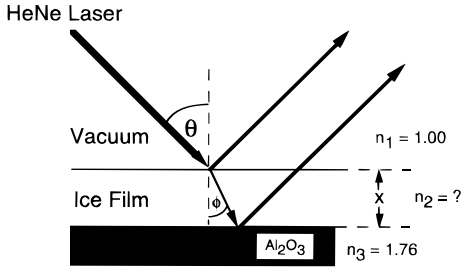

Figure 4. Geometric representation of the optical interference technique.

160 K. The ice film was then annealed to higher temperatures using a series of small temperature ramps. During each temperature ramp, the partial pressure of H_2O was adjusted to maintain a steady-state film thickness as determined by optical interference measurements.[15]

The H_2O partial pressures over the ice films at steady state were measured with the ionization gauge that had been previously calibrated using the absolute capacitance manometer. The H_2O vapor was taken from a reservoir of distilled and deionized water. The water reservoir was purified with several liquid nitrogen freeze−pump−thaw cycles. The H_2O partial pressures used in this study ranged from 1×10^{-6} to 4×10^{-4} Torr.

High partial pressures of H_2O were required to prevent the ice films from desorbing at the higher ice temperatures. At higher H_2O pressures, the H_2O background signal in the mass spectrometer is large, and the operational dynamic range is reduced by the upper limit of the preamplifier of the electron multiplier. Consequently, H_2O was detected using the smaller intensity H_2O cracking fragment at $m/e = 17$, corresponding to OH^+ for most of the experiments. Experiments that required even higher H_2O pressures utilized the H_2O cracking fragment at $m/e = 16$, which is the smallest peak of the cracking pattern.

Once the ice film was prepared, hydrogen chloride gas (Aldrich, 99+% anhydrous) was backfilled into the chamber. The HCl pressures ranged from 1×10^{-9} to 2×10^{-6} Torr. The HCl partial pressures were measured with the quadrupole mass spectrometer. The mass spectrometer was calibrated versus the ionization gauge. The ionization gauge was previously calibrated using the absolute capacitance manometer. HCl was detected using the parent, HCl^+, at mass $m/e = 36$.

C. Optical Interference To Determine Film Thickness. Optical interference methods were used to measure the steady-state ice film thickness and to determine the real refractive index of the HCl hydrates.[15] For the interference technique, a helium−neon (HeNe) laser at $\lambda = 6328$ Å impinges on a growing ice film at near normal incidence. Figure 4 presents a schematic view of the reflectance geometry. Part of the HeNe laser beam is reflected by the vacuum−ice interface. Some of the HeNe light is reflected from the ice−Al_2O_3 interface.

As the film grows, the two reflected beams interfere with each other and produce a sinusoidal interference pattern. The intensity of the reflected beam is measured using a photomultiplier tube (Hamamatsu R928). The ice film thickness, x, is then obtained using

$$x = m\lambda/2n(T) \qquad (2)$$

where m is the number of periods of oscillation, and $n(T)$ is the temperature-dependent refractive index of the ice film.[26]

The reflectance of the HeNe laser from a growing ice film at 140 K is shown in Figure 5a. The reflectance during the codeposition of H_2O and HCl at 140 K is shown in Figure 5b. A comparison of parts a and b reveals that the minimum

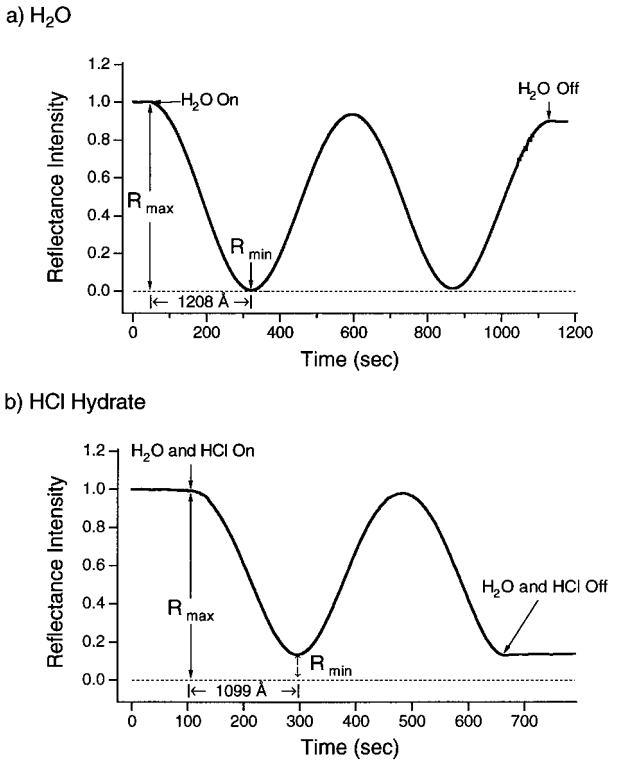

Figure 5. Typical optical interference data for (a) H_2O ice films and (b) HCl hydrate films deposited on the Al_2O_3 substrate at 140 K. Using the measured refractive indices, one-half of an optical cycle corresponds to 1208 Å in (a) and 1099 Å in (b).

reflectance (R_{min}) in Figure 5b is significantly higher than the R_{min} in Figure 5a. These differences are caused by different refractive indices for the two films.

The real refractive index of the deposited film can be determined by analyzing the optical interference data using Fresnel's equations.[26,27] Briefly, the Fresnel equations indicate that the ratio between the minimum and maximum reflectance values is

$$\frac{R_{min}}{R_{max}} = \frac{[(n_1 n_3 - n_2^2)/(n_1 n_3 + n_2^2)]^2}{[(n_1 - n_3)/(n_1 + n_3)]^2} \qquad (3)$$

The refractive index of the Al_2O_3 substrate is $n_3 = 1.76$, the refractive index of vacuum is $n_1 = 1.00$, and n_2 is the refractive index of the film. Consequently, the ratio R_{min}/R_{max} measured during film growth can be used to determine the refractive index of the ice or HCl hydrate film.

In this study, the measured refractive index for a pure water ice film was $n = 1.31$ at 140 K. This index is in excellent agreement with previous optical interference measurements[26] and the literature value of $n = 1.31$ at 266 K.[28] Codeposition of HCl and H_2O at 140 K resulted in an HCl trihydrate film with a refractive index of $n = 1.44$. With these refractive indices employed in eq 2, one half-cycle of oscillation for a pure ice film corresponds to an ice film thickness of $x = 1208$ Å. Likewise, one half-cycle of oscillation for the HCl trihydrate corresponds to a thickness of $x = 1099$ Å.

D. Laser-Induced Thermal Desorption To Determine Film Composition. Laser-induced thermal desorption (LITD) measurements were used to determine the composition of the HCl and H_2O films as a function of HCl partial pressure, film temperature, and film thickness.[29−31] For the LITD investigations, a pulsed Lumonics CO_2 TEA laser at $\lambda = 10.6$ μm was modified for TEM-00 operation.[32] The laser beam was first

expanded to a diameter of 2 cm with a ZnSe beam expander. The beam was then focused to a diameter of <1 mm on the Al_2O_3 substrate using a 75 cm focal length ZnSe lens. The CO_2 laser beam entered the chamber through a ZnSe window and impinged on the Al_2O_3 substrate at 45° from the surface normal as shown in Figure 2.

The CO_2 radiation is absorbed by a localized area of the adsorbed multilayer and the underlying Al_2O_3 substrate.[26] This laser heating results in the rapid thermal desorption of the illuminated multilayer. The CO_2 laser energies used in this experiment were between 45 and 70 mJ/pulse. Using the autocorrelation method,[33] the laser desorption area had a diameter of ~715 μm for the HCl hydrates and ~600 μm for the pure ice films.

High sensitivity is required to detect submonolayer HCl coverage on ice under stratospheric conditions. To enhance the surface sensitivity, the ionizer of the mass spectrometer was positioned with direct line-of-sight to the multilayer on the Al_2O_3 substrate. The surface normal at the center of the Al_2O_3 substrate was aligned with the center line of the glass shroud, the copper cryopanel, and the mass spectrometer ionizer as shown in Figure 2. This orientation permitted the surface species to desorb from the Al_2O_3 crystal and directly travel to the ionizer of the mass spectrometer. This desorption signal arrives in advance of the pressure burst that equilibrates within the vacuum chamber.[26] Line-of-sight detection of the surface species provides a direct probe of the surface coverage and allows the surface species to be detected with submonolayer sensitivity.

To calibrate LITD signals, vapor is deposited onto the Al_2O_3 substrate, and optical interference is used to measure the multilayer film thickness during film growth. LITD signals for H_2O have been successfully calibrated using this technique in previous studies.[26] LITD signals were recorded for ice films with various thicknesses. Film thickness (Å) was converted to H_2O coverage (molecules/cm^2) using the known density (g/cm^3) and molecular weight (g/mol) of the ice film. Because the correlation between H_2O LITD signals and H_2O coverage was linear, the H_2O coverage in unknown films was determined from the H_2O LITD signals.[26]

A slight variation was applied to the above calibration procedure to determine the HCl and H_2O coverages from the HCl and H_2O LITD signals in this study. Pure HCl multilayers are not stable in vacuum at liquid nitrogen temperatures, and the HCl LITD signal could not be calibrated using pure HCl films. For this reason, mixed HCl/H_2O films were used to calibrate the HCl LITD signals. H_2O and HCl vapor were codeposited onto the Al_2O_3 substrate at 140 K with an H_2O partial pressure of $\sim 1 \times 10^{-6}$ Torr and an HCl partial pressure of $\sim 5 \times 10^{-7}$ Torr. The LITD signals of HCl ($m/e = 36$) and H_2O ($m/e = 16$) were then recorded for each film. The HCl/H_2O LITD signal ratios were consistently the same for these films. This behavior indicates that a reproducible and stable HCl hydrate formed by the codeposition of HCl and H_2O under these conditions.

Gas phase calibrations of H_2O ($m/e = 16$) and HCl ($m/e = 36$) were used to determine the composition of the hydrate film at 140 K. Differential pumping was not used during these calibration experiments to ensure that the pressure measured by the capacitance manometer was the same as the pressure measured by the ionizer of the mass spectrometer. The ionization gauge was first calibrated using the absolute capacitance manometer at HCl and H_2O pressures of 4×10^{-6}–3×10^{-4} Torr. Subsequently, the calibrated ionization gauge was used to determine the relative mass spectrometer sensitivity for each gas at pressures of 7×10^{-8}–3×10^{-4} Torr. The UTI 100C mass spectrometer was found to be 36 times more sensitive to HCl at $m/e = 36$ than to the cracking fragment of H_2O at $m/e = 16$.

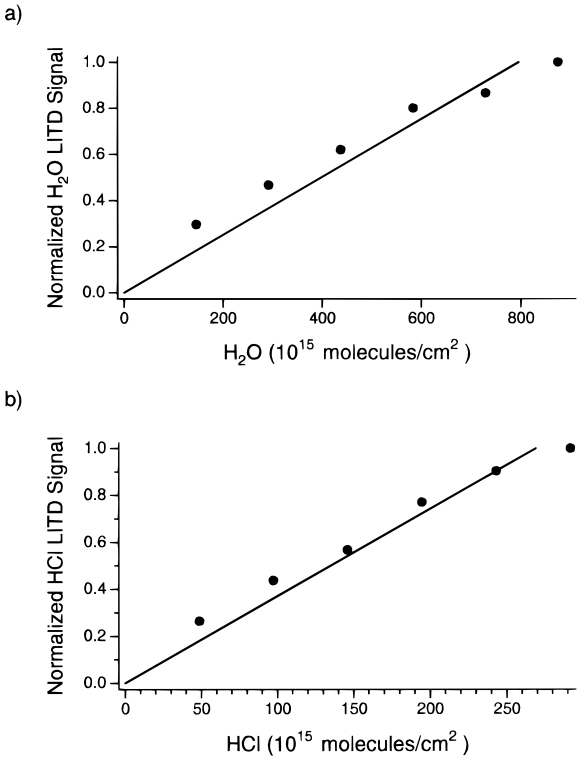

Figure 6. Calibration of the H_2O and HCl LITD signals versus surface coverage. Codeposition of HCl and H_2O vapor at 140 K formed the HCl·3H_2O trihydrate that was used to calibrate the LITD signals.

The relative mass spectrometer sensitivities were then used to calibrate the LITD signals and determine the stoichiometry of the HCl hydrate deposited at 140 K. The calibrated HCl and H_2O LITD signals indicated that the HCl/H_2O film formed by codeposition at 140 K was an HCl·3H_2O trihydrate. LITD signals for HCl and H_2O were then measured for various thicknesses of the HCl·3H_2O film. The H_2O LITD signal is plotted as a function of H_2O coverage (molecules/cm^2) in Figure 6a. Similarly, the HCl LITD signal is plotted versus the HCl coverage (molecules/cm^2) in Figure 6b.

The plots of HCl and H_2O LITD signals versus HCl and H_2O surface coverages are linear. Because the correlations are linear, the HCl and H_2O coverages in an unknown HCl/H_2O film can be determined using the HCl and H_2O LITD signals. The calibration results for H_2O using the HCl·3H_2O trihydrate are in reasonable agreement with the calibration of the H_2O LITD signals using the pure ice multilayers.[26] LITD calibrations using the HCl·3H_2O trihydrate were repeated daily to account for any possible drift in the mass spectrometer sensitivity.

3. Results

A. HCl Trihydrate at 140 K. Thin films of H_2O were initially deposited onto the Al_2O_3 substrate at 140 K to produce an ice film thickness of 520 ± 36 Å. The ice films were then exposed to HCl partial pressures ranging from 3×10^{-8} to 7×10^{-7} Torr. During the HCl exposures, LITD signals were recorded to measure the change in the HCl concentration in the ice film versus time. Figure 7 shows the HCl concentrations in the ice films rising rapidly to form a saturated and stable HCl hydrate. In every case, a reproducible HCl hydrate was obtained within the first 20 min of HCl exposure to the ice film.

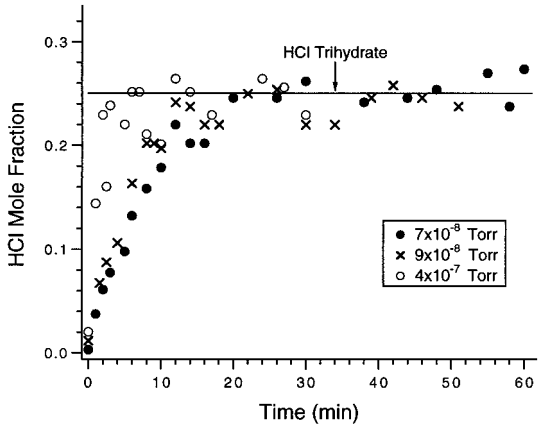

Figure 7. HCl mole fraction of ice films at 140 K as a function of HCl exposure time at various HCl pressures. The initial ice films had a thickness of 520 ± 36 Å.

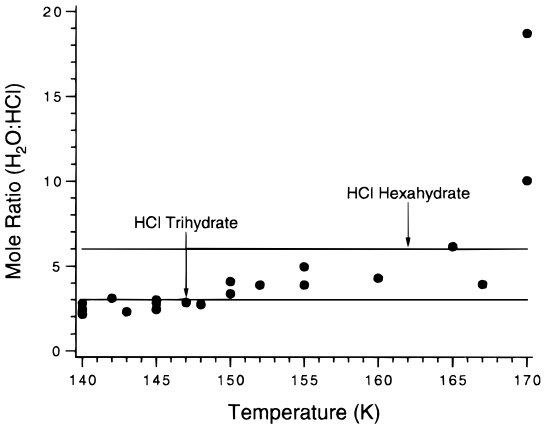

Figure 8. Saturated H_2O:HCl mole ratio for ice films exposed to HCl pressure as a function of substrate temperature between 140 and 170 K.

Ice films exposed to higher pressures of HCl formed the HCl hydrate more quickly than ice films exposed to lower HCl pressures.

The mole fraction of HCl in the HCl/H_2O films in Figure 7 was calculated from the measured HCl and H_2O LITD signals. These LITD signals were calibrated using the relative mass spectrometer sensitivities determined from the gas phase calibrations. The measured mole fraction of HCl in the saturated ice film was 0.25 ± 0.02. This stoichiometry indicates the formation of an HCl·$3H_2O$ trihydrate. The HCl trihydrate formed for all the temperatures investigated between 140 and 148 K. These conditions are well within the expected stability region for the HCl trihydrate according to the HCl/H_2O phase diagram shown in Figure 1. The agreement between the LITD experimental results and the phase diagram supports the assignment of these saturated HCl/H_2O films at 140−148 K as HCl·$3H_2O$ trihydrate.

B. 150−170 K: Variable Compositions. In contrast to the observation of HCl·$3H_2O$ between 140 and 148 K, the interaction of HCl with ice in the temperature range from 150 to 170 K gave notably different results. Although these ice films displayed saturation behavior with respect to HCl, they did not saturate at a 3:1 H_2O:HCl mole ratio. The H_2O:HCl mole ratio for these films versus film temperature is shown in Figure 8. The HCl and H_2O LITD calibrations utilized the HCl·$3H_2O$ trihydrate formed by codeposition at 140 K. From 150 to 170 K, the HCl concentration in the saturated film decreased progressively as a function of temperature. Because no fixed composition is established, nonstoichiometric amorphous solid solutions or polycrystalline hydrates are believed to be forming in this temperature range.

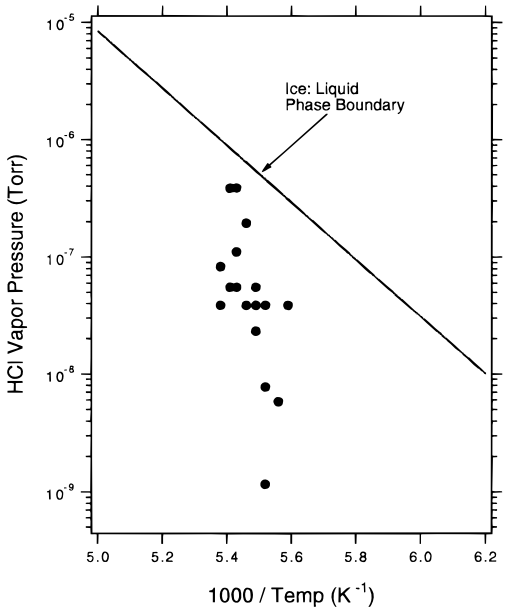

Figure 9. HCl partial pressures and substrate temperatures used in the experiments performed under stratospheric conditions that are shown in Figure 10. The ice:liquid phase boundary is determined from ref 9.

C. 179−186 K: Stratospheric Conditions. The HCl partial pressures and temperatures employed in HCl uptake experiments that simulate the stratospheric region are plotted in Figure 9. The solid line represents the ice:liquid coexistence line as determined by vapor pressure measurements over equilibrium mixtures of liquid HCl solution and ice.[9] All of the experimental points fall well below the ice:liquid line. Consequently, these HCl uptake measurements should represent HCl on ice and not on an H_2O liquid layer.

LITD analysis was used to measure the HCl coverage on or in the ice films at stratospheric conditions. Two types of ice films were prepared for these experiments. In one set of experiments, H_2O vapor was deposited on the Al_2O_3 substrate at ≈183 K prior to the HCl exposures. In the other set of experiments, ice films were first deposited onto the Al_2O_3 substrate at a lower substrate temperature of 160 K. Subsequently, the films were annealed to stratospheric temperatures using $\Delta T \sim 2$ K increments prior to HCl exposure.

For ice films prepared at 183 K, the saturated HCl coverage was found to be $(7.3 \pm 1.6) \times 10^{15}$ molecules/cm^2. The error bars on this measurement represent the typical scattering observed in the HCl LITD signal. This scattering is attributed to shot-to-shot laser pulse energy variations and slight film inhomogeneities. If the ice surface is the basal plane of hexagonal ice, the number of H_2O surface sites on the top bilayer of ice is 1.15×10^{15} molecules/cm^2.[34] Using this coverage as a reference point to represent a one monolayer coverage (1 ML $= 1.15 \times 10^{15}$ molecules/cm^2), the HCl surface coverage is $\Phi_{HCl} = 6.3 \pm 1.4$ ML on ice at 183 K. This HCl coverage is higher than the near monolayer coverage reported in previous studies.[9,10,18,22]

Although theoretical calculations have not predicted the expected HCl coverages on ice under stratospheric conditions,[12−15,19] experimental investigations measure HCl coverages $8 \times 10^{13}-3 \times 10^{15}$ molecules/cm^2 [9,10,18,22] or 0.1−3 ML. HCl coverages higher than 1 ML may be caused by surface roughness on the ice film. To attempt to decrease the roughness of ice surfaces, the ice films were first deposited at 160 K and then annealed to stratospheric temperatures between 180 and 186

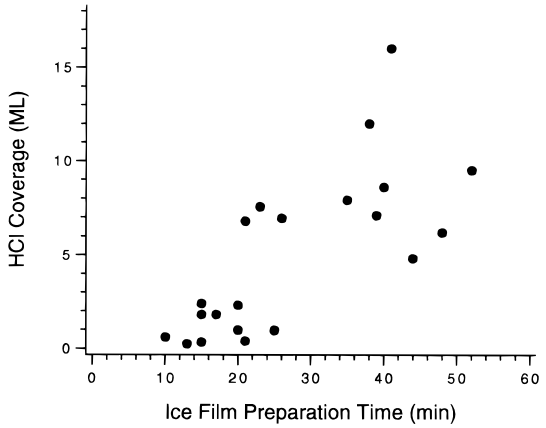

Figure 10. HCl coverage on the ice films under stratospheric conditions versus ice film preparation time. The HCl partial pressures and substrate temperatures are given in Figure 9.

K. This method has previously been shown to produce smoother films than those formed by direct deposition at high temperatures.[35] During annealing, the H_2O vapor pressure was adjusted simultaneously to prevent ice film growth or evaporation. Optical interference measurements were utilized to monitor the ice film thickness and to attempt to keep the ice film at steady state and a constant thickness during the annealing process.

The annealed ice films were then exposed to HCl partial pressures between 1×10^{-9} and 5×10^{-7} Torr. The HCl LITD signals were measured and consistent HCl LITD signals were observed after HCl exposure time of $\gtrsim$3 min. The measured HCl coverage on the annealed ice films varied greatly from 4×10^{14} to 2×10^{16} molecules/cm^2 or 0.4 to 16.2 ML. Despite this large range of HCl coverages, there was no observed correlation between the HCl coverage and either the ice film temperature or the HCl partial pressures. The experimental scatter of the HCl LITD signal for an individual experiment is much too low to explain this large range of HCl coverages.

The HCl coverages did correlate roughly with the total preparation time before the ice films were exposed to HCl vapor. Ice film preparation time includes the time required to deposit the films at 160 K, to anneal the film to above 180 K, and to determine that the films were at steady state and a constant thickness. The measured HCl coverage is plotted as a function of the total ice preparation time prior to HCl exposure in Figure 10. The highest HCl coverages were measured for the ice films that required the longest preparation times. This correlation between measured HCl coverage and ice film preparation time can be explained if the ice films roughen versus preparation time.

4. Discussion

A. HCl Trihydrate Regime at 140 K. The HCl·3H_2O trihydrate was observed to form when HCl interacts with ice films at temperatures between 140 and 148 K. The HCl·3H_2O trihydrate formed over a wide range of HCl partial pressures as shown in Figure 7. The trihydrate was very stable and clearly establishes a 1:3 HCl:H_2O stoichiometry. This behavior is expected on the basis of the HCl/H_2O phase diagram shown in Figure 1.

A second check on the identity of the HCl hydrate as HCl·3H_2O can be obtained using optical interference measurements of the real refractive index. An index of refraction for the HCl·3H_2O hydrate can be calculated using the Lorentz−Lorenz relationship. The Lorentz−Lorenz relationship is based on the molar refractivity of the components of a mixture, the molecular weight of the mixture, and the density of the mixed film:[26,27,36]

$$A = \frac{w(n^2 - 1)}{\rho(n^2 + 2)} \tag{4}$$

The Lorentz−Lorenz relationship has been shown to predict the refractive index very well for amorphous HNO_3/H_2O films.[26]

The molar refractivity of a 40 wt % HCl solution, i.e., a 3:1 H_2O:HCl solution, was used in the calculation of the refractive index. Based on the molecular weight of 90.5 g/mol, a density of 1.20 g/cm^3, and a refractive index of $n = 1.42$ at 293 K,[37] a molar refractivity of $A = 19.3$ cm^3/mol was determined for the 40 wt % HCl solution. A density of $\rho = 1.24$ g/cm^3 was obtained for the HCl·3H_2O trihydrate film at 140 K by extrapolating density versus temperature data available at higher temperatures.[38] Using the molar refractivity of $A = 19.3$ cm^3/mol at 293 K and density of $\rho = 1.24$ g/cm^3 at 140 K, the refractive index obtained from the Lorentz−Lorenz relationship for an HCl·3H_2O film at 140 K is $n = 1.44$.

The refractive index can be measured using optical interference techniques and compared with the predicted refractive index of HCl·3H_2O obtained using the Lorentz−Lorenz relationship.[26,27] HCl hydrate films were deposited by simultaneously backfilling a mixture of HCl and H_2O vapor onto a cooled Al_2O_3 substrate at 140 K. The real refractive index of the HCl hydrate formed during deposition was then determined from the optical interference data collected during film growth.[26,27] The index of refraction was measured to be $n = 1.44$ for each experiment conducted at 140 K. This excellent agreement is additional confirmation of the assignment of the hydrate as HCl·3H_2O trihydrate.

A recent temperature-programmed desorption (TPD) study has also been employed to evaluate ice films exposed to HCl at 120 K.[20] After saturation HCl exposures, the reported film composition was HCl·6H_2O hexahydrate. This assignment was based on integrated TPD signals that were calibrated using literature values for HCl and H_2O ionization efficiencies.[39] However, there is uncertainty in this assignment because the relative ionization efficiencies for HCl and H_2O were not known with great accuracy.[20] Consequently, the discrepancy between these TPD studies and the present LITD investigation may be ascribed to calibration difficulties.

B. Variable Compositions between 150 and 170 K. According to the phase diagram in Figure 1, some of the experimental conditions used in this experiment include the predicted region for the HCl hexahydrate (HCl·6H_2O). However, Figure 8 shows that a stoichiometric HCl·6H_2O was not observed as a stable phase over an appreciable temperature range. A stable HCl·3H_2O phase was observed between 140 and 148 K. Above 150 K, HCl concentrations continuously decreased with increasing substrate temperature.

Although a stable HCl·6H_2O hexahydrate was not observed under the conditions in this experiment, these results may reflect the difficulty in nucleating the hexahydrate phase. The hexahydrate phase has been reported earlier, but many of these studies utilized infrared spectra for identification.[9,17,21,40,41] The differences between the LITD measurements and the previous infrared work may be attributed to inconstancies in the assignment of the infrared spectra for the various HCl hydrates. All of the FTIR assignments result from earlier assignments for the infrared spectra of HCl·4H_2O and HCl·6H_2O.[40] If these earlier spectra were incorrectly assigned, all the subsequent assignments based on these spectra may require reevaluation.

In other studies, HCl hydrates were formed by freezing HCl/H_2O solutions.[42,43] These studies did not produce HCl hexahydrate even when the HCl·6H_2O was favored state according to the phase diagram. HCl·6H_2O was formed only when solutions

were frozen to lower temperatures and then annealed to the stability region of $HCl{\cdot}6H_2O$. Consequently, there may be a nucleation barrier for $HCl{\cdot}6H_2O$ formation that may have precluded the observation of a stable hexahydrate in these and our studies.

C. HCl Interaction with Ice under Stratospheric Conditions. The ice films deposited at 183 K prior to the HCl exposures yielded a saturation HCl coverage of $(7.3 \pm 1.6) \times 10^{15}$ molecules/cm^2 or 6.3 ± 1.4 ML. This HCl coverage is greater than the 0.1−3 ML HCl uptake by ice at stratospheric temperatures reported by earlier experiments.[9,10,18,22] Some of the differences may be explained if the experimental surface area of the ice films in the present study are greater than the geometric surface area of the Al_2O_3 substrate. Under stratospheric conditions, water molecules are continuously adsorbing and desorbing from the ice surface.[15] This dynamic ice surface may lead to substantial surface roughening.

Scanning electron micrographs and BET adsorption measurements show that ice films are extremely rough when prepared using direct vapor deposition.[44] Other experimental studies have also observed surface roughening of ice films as a function of time.[35] In addition, various theoretical models are consistent with surface roughening versus time during film growth. For example, a recent Monte Carlo analysis[45] observed that the surface of a film became increasingly rough as the film grew at high temperatures.

Ice films were deposited at lower temperatures of 160 K and then progressively annealed to stratospheric temperatures to attempt to minimize surface roughness. The results of these experiments are shown in Figure 10. A wide range of HCl coverages were measured ranging from ∼1 ML to over 16 ML. However, the larger HCl coverages were consistently measured after longer ice film preparation times. These results suggest that the ice films are roughening versus film preparation time. At the shortest ice film preparation times, the HCl coverage is ∼1 ML. These ice films are presumably the smoothest films and the closest approximation to an ice film with a surface area equivalent to the Al_2O_3 substrate.

The surface coverage of HCl on ice under stratospheric conditions is best represented by the uptake of HCl on the smoothest ice surfaces. The smoothest ice surfaces are most likely the annealed ice films prepared in less than 15 min. Assuming that the surface area of these ice films is equivalent to the geometric surface area of the Al_2O_3 substrate, the HCl coverage on ice corresponds to ∼1 ML.

An HCl coverage of ∼1 ML is in agreement with the near monolayer HCl surface coverage measured in previous flow tube studies at stratospheric temperatures.[9,10,18] In these earlier flow tube investigations, the surface area of the ice film on the tube was assumed to be equivalent to the geometrical surface area. The present study suggests that the surface area of the ice film should depend on preparation conditions and preparation time. The exact surface area of the ice films in the flow tube experiments is not known. Consequently, the agreement between these HCl LITD measurements and the flow tube experiments may be fortuitous.

The saturation HCl coverage on the smoothest ice films is ∼1 ML. This saturation coverage is independent of the HCl pressure over a pressure range from 10^{-9} to 10^{-6} Torr. Consequently, the rate of heterogeneous reaction given in eq 1 should be independent of P_{HCl} if enough HCl pressure is present to form ∼1 ML HCl coverage. This constant HCl saturation coverage may explain the observation of equal rates for the reaction given in eq 1 for HCl pressures that vary by a factor of 100.[46]

5. Conclusions

The interaction of HCl with ice was studied as a function of ice temperature and HCl partial pressure using laser-induced thermal desorption (LITD) techniques. In agreement with the HCl/H_2O phase diagram, a stable $HCl{\cdot}3H_2O$ trihydrate consistently formed between 140 and 148 K. Between 150 and 170 K, the $HCl{:}H_2O$ ratio changed continuously versus temperature, and no special stability was observed for the $HCl{\cdot}6H_2O$ hexahydrate. Under stratospheric conditions, the uptake of HCl by ice varied from 0.4 to 16.2 ML (1 ML = 1.15×10^{15} molecules/cm^2). The variation in the measured HCl coverages scaled approximately with ice film preparation time. These results suggest that the ice films roughen versus film preparation time under stratospheric conditions. On the smoothest ice films, the HCl coverage is ∼1 ML and independent of HCl pressure from 10^{-9} to 10^{-6} Torr. These results indicate that HCl is readily available on ice surfaces for heterogeneous reaction in the polar stratosphere.

Acknowledgment. This research was supported by grants from the National Science Foundation (CHE-9528473 and ATM-9321582) and NASA (SASS-94-091). K.L.F. acknowledges the David and Lucile Packard Foundation for the receipt of a Scholars Program in Chemistry, Physics and Math Fellowship. M.A.T. was supported as an NSF Young Investigator Award and a Camille Dreyfus Teacher Scholar. The authors are also grateful to Prof. M. J. Molina for permitting the use of the phase diagram shown in Figure 1.

References and Notes

(1) Solomon, S. *Nature* **1990**, *347*, 347.
(2) *WMO Global Ozone Research and Monitoring Project—Report No. 37 Scientific Assessment of Ozone Depletion: 1994*; World Scientific Publishing: Singapore, 1995.
(3) Turco, R. P.; Toon, O. B.; Hamill, P. *J. Geophys. Res.* **1989**, *94*, 16493.
(4) Vömel, H.; Hofmann, D. J.; Oltmans, S. J.; Harris, J. M. *Geophys. Res. Lett.* **1995**, *22*, 2381.
(5) Solomon, S. *Rev. Geophys.* **1988**, *26*, 131.
(6) Molina, L. T.; Molina, M. J.; Stachnik, R. A.; Tom, R. D. *J. Phys. Chem.* **1985**, *89*, 3779.
(7) Tolbert, M. A.; Rossi, M. J.; Malhotra, R.; Golden, D. M. *Science* **1987**, *238*, 1258.
(8) Molina, M. J.; Tso, T.-L.; Molina, L. T.; Wang, F. C.-Y. *Science* **1987**, *238*, 1253.
(9) Abbatt, J. P. D.; Beyer, K. D.; Fucaloro, A. F.; McMahon, J. R.; Wooldridge, P. J.; Zhang, R.; Molina, M. J. *J. Geophys. Res.* **1992**, *97*, 15819.
(10) Hanson, D. R.; Ravishankara, A. R. *J. Phys. Chem.* **1992**, *96*, 2682.
(11) Molina, M. J. The Probable Role of Stratospheric "Ice" Clouds: Heterogeneous Chemistry of the "Ozone Hole". In *The Chemistry of the Atmosphere: Its Impact on Global Change*; Calvert, J. G., Ed.; Blackwell Scientific: Boston, MA, 1994; p 27.
(12) Kroes, G.-J.; Clary, D. C. *Geophys. Res. Lett.* **1992**, *19*, 1355.
(13) Robertson, S. H.; Clary, D. C. *Faraday Discuss. Chem. Soc.* **1995**, *100*, 309.
(14) Gertner, B. J.; Hynes, J. T. *Science* **1996**, *271*, 1563.
(15) Haynes, D. R.; Tro, N. J.; George, S. M. *J. Phys. Chem.* **1992**, *96*, 8502.
(16) Horn, A. B.; Chesters, M. A.; McCoustra, M. R. S.; Sodeau, J. R. *J. Chem. Soc., Faraday Trans.* **1992**, *88*, 1077.
(17) Koehler, B. G.; McNeill, L. S.; Middlebrook, A. M.; Tolbert, M. A. *J. Geophys. Res.* **1993**, *98*, 10563.
(18) Chu, L. T.; Chu, L. T.; Leu, M.-T.; Keyser, L. F. *J. Phys. Chem.* **1993**, *97*, 7779.
(19) Wolff, E. W.; Mulvaney, R.; Oates, K. *Geophys. Res. Lett.* **1989**, *16*, 487.
(20) Graham, J. D.; Roberts, J. T. *J. Phys. Chem.* **1994**, *98*, 5974.
(21) Banham, S. F.; Horn, A. B.; Koch, T. G.; Sodeau, J. R. *Faraday Discuss. Chem. Soc.* **1995**, *100*, 321.
(22) Dominé, F.; Thibert, E.; Chaix, L. Interactions of Gas Phase HCl and HNO_3 with Ice. In *Chemical Exchange Between the Atmosphere and Polar Snow*; Wolff, E. W., Bales, R. C., Eds.; Springer: Verlag, 1996; Vol. 143, p 567.

(23) Tro, N. J.; Haynes, D. R.; Nishimura, A. M.; George, S. M. *J. Phys. Chem.* **1989**, *93*, 3276.

(24) Tro, N. J.; Haynes, D. R.; Nishimura, A. M.; George, S. M. *J. Phys. Chem.* **1989**, *91*, 5778.

(25) Brown, D. E.; George, S. M.; Huang, C.; Wong, E. K. L.; Rider, K. B.; Smith, R. S.; Kay, B. D. *J. Phys. Chem.* **1996**, *100*, 4988.

(26) Berland, B. S.; Haynes, D. R.; Foster, K. L.; Tolbert, M. A.; George, S. M.; Toon, O. B. *J. Phys. Chem.* **1994**, *98*, 4358.

(27) Born, M.; Wolf, E. *Principles of Optics*; Pergamon Press: Oxford, 1975.

(28) Warren, S. G. *Appl. Opt.* **1984**, *23*, 1206.

(29) George, S. M. Laser Induced Thermal Desorption. In *Investigations of Surfaces and Interfaces—Part A*, 2nd ed.; Rossiter, B. W., Baetzold, R. C., Eds.; John Wiley & Sons: New York, 1993; Vol. IXA, p 453.

(30) Mak, C. H.; Brand, J. L.; Deckert, A. A.; George, S. M. *J. Chem. Phys.* **1986**, *85*, 1676.

(31) Hall, R. B.; DeSantolo, A. M. *Surf. Sci.* **1984**, *137*, 421.

(32) Arthur, D. A.; Meixner, D. L.; Boudart, M.; George, S. M. *J. Chem. Phys.* **1991**, *95*, 8521.

(33) George, S. M.; DeSantolo, A. M.; Hall, R. B. *Surf. Sci. Lett.* **1985**, *159*, L425.

(34) Pruppacher, H. R.; Klett, J. D. *Microphysics of Clouds and Precipitation*; D. Reidel Publishing: Dordrecht, Holland, 1978.

(35) Middlebrook, A. M.; Berland, B. S.; George, S. M.; Tolbert, M. A.; Toon, O. B. *J. Geophys. Res.* **1994**, *99*, 25.

(36) Heavens, O. S. *Optical Properties of Thin Solid Films*; Dover Publications: New York, 1991.

(37) *CRC Handbook of Chemistry and Physics*, 66th ed.; Weast, R. C., Ed.; CRC Press: Boca Raton, FL, 1985; p D232.

(38) *Chemical Engineer's Handbook*, 2nd ed.; Perry, J. H., Ed.; McGraw-Hill Book Co.: New York, 1941; p 417.

(39) Cornu, A.; Massot, R. *Compilation of Mass Spectral Data*; Heyden: London, 1966.

(40) Ritzhaupt, G.; Devlin, J. P. *J. Phys. Chem.* **1991**, *95*, 90.

(41) Delzeit, L.; Rowland, B.; Devlin, J. P. *J. Phys. Chem.* **1993**, *97*, 10312.

(42) Hanson, D. R.; Mauersberger, K. *J. Phys. Chem.* **1990**, *94*, 4700.

(43) Wooldridge, P. J.; Zhang, R.; Molina, M. J. *J. Geophys. Res.* **1995**, *100*, 1389.

(44) Keyser, L. F.; Leu, M. T. *Microsc. Res. Technol.* **1993**, *25*, 434.

(45) Xiao, R.-F.; Ming, N.-B. *Phys. Rev. E* **1994**, *49*, 4720.

(46) Hanson, D. R.; Ravishankara, A. R. *J. Geophys. Res.* **1993**, *98*, 22.